Even- and Odd-Mode Analysis of Thick and Wide Slot in Waveguides Based on a Variational Method

Wang Wenzhi, Ye Sheng, Liang Xianling, Jin Ronghong, Trevor S. Bird, *Fellow, IEEE*, Y. Jay Guo, *Senior Member, IEEE*, Geng Junping

***Abstract*— Based on a new variational method, an even- and odd-mode analysis of broadwall coupling slot between waveguides is presented. The proposed method is capable of dealing with the effect of finite wall thickness. It uses multiple incident waves with symmetry to simplify the field distribution in the vicinity of the slot, enabling the adoption of one-expansion-term trial functions with sufficient accuracy, even in the instance of wide slots. Analytical solutions are provided, and the calculated results demonstrate excellent agreement with those of HFSS. The computation time with the new formulation is, however, significantly shorter.**

***Index Terms*— variational method, coupling slots, even- and odd-mode analysis, wide slots, finite wall thickness**

I. Introduction

WAVEGUIDE slot couplers are in widespread use for many significant applications. Over the years, a variety of methods have been developed for analyzing the properties of slots in waveguides. In one approach, Stevenson [1] developed a rigorous method for calculating the scattering parameters of coupling slots near resonance. Later, Lewin [2] and Pandharipande [3] proposed approximate methods based on similar ideas in which slots were treated as equivalent antennas. Sangster [4] applied a variational method to the analysis of single transverse slots, through which a good balance was achieved between accuracy and complexity. The most attractive advantage of the above methods is the existence of analytical solutions, which are valuable for practical design and optimization. However, their assumption of zero wall thickness limits their usefulness in certain situations. In addition, numerical techniques such as the method of moments (MoM) [5]-[7], finite-difference time domain method [8], [9], the finite-element method [10], and the mode-matching method [11]-[13] can be used to analyze slotted waveguide with finite wall thickness to great practical accuracy. Compared with analytical methods, however, greater programming effort and execution time are required, which can be prohibitive for large scale problems that may require adaptive optimization.

When the coupling slot is considered from the point of view of scattering in waveguides, most existing methods employ single wave incidence as a precondition for analysis [4]-[7]. For instance, the analysis of slotted rectangular waveguide directional coupler is usually based on a single TE_{10} mode incident from one of the four ports. The slot properties can then be obtained by describing the field distribution around the slot area, which is usually achieved by selected basis function expansion. Previous work has shown that this is an effective way of analyzing narrow slot problems. However, when considering wide slots, more expansion terms are required to represent the complex field distribution in the vicinity of wide slots. In this case, solutions obtained from the current analytical methods are often too complex to be practical. Therefore, their use is normally limited to narrow slots, usually with aspect ratio greater than ten.

Based on a variational method, an even- and odd-mode analysis is described in this paper, which provides analytical solutions of scattering parameters of a wide transverse slot with finite wall thickness in the common broad wall of two rectangular waveguides. The proposed method employs multiple incident waves with symmetry to simplify the field distribution in the vicinity of the slot, enabling the adoption of one-expansion-term trial functions with sufficient accuracy even for wide slots. The paper is organized as follows. In Section II, the theory is described, including the derivation of a variational expression, the selection of trial functions and solutions of

Manuscript received March 1, 2012. This work was supported by "973" (2009CB320403), the Natural Science Foundation of Shanghai under Grant (10ZR1416600), the Doctoral Fund of Ministry of Education of China under Grant (20090073120033), the National Science and Technology Major Project of the Ministry of Science (2011ZX03001-007-03), the National Science Fund for Creative Research Groups under Grant (60821062) and the Scientific Research Foundation for the Returned Overseas Chinese Scholars, State Education Ministry.

Wang Wenzhi, Ye Sheng, Liang Xianling, Jin Ronghong and Geng Junping are with the Department of Electronic Engineering, Shanghai Jiao Tong University, Shanghai, China (e-mail: simonary@sjtu.edu.cn; zqntoys@sjtu.edu.cn; liangxl@sjtu.edu.cn; rhjin@sjtu.edu.cn; gengjunp@sjtu.edu.cn).

Trevor S. Bird and Y. Jay Guo are with CSIRO, Sydney, Australia (e-mail: ts.bird@ieee.org; Jay.Guo@csiro.au).

scattering parameters. Computed results from this formulation are presented in Section III and these are compared with data obtained from HFSS. The results are also discussed in Section IV, which is followed by a conclusion in Section V.

II. Theory

A. Derivation of Variational Expression

The geometry of a transverse slot in the common broad wall of two rectangular waveguides is shown in Fig. 1. For simplification, the original problem is transformed using the equivalence principle into an equivalent one through region division [5], [7]. As depicted in Fig. 2, the region division is performed by placing two electric walls at interfaces S_1 and S_2. Each electric wall is appended with two sheets on either side with magnetic currents $\boldsymbol{J}^{+}_{\mathrm{M}_i} = \boldsymbol{a}_y \times \boldsymbol{E}_{S_i}$ and $\boldsymbol{J}^{-}_{\mathrm{M}_i} = -\boldsymbol{a}_y \times \boldsymbol{E}_{S_i}$, where $\boldsymbol{E}_{S_i}$ is the electric field on S_i in the original waveguide, i = 1, 2. Therefore, the slot area is divided into 3 regions. According to the continuity conditions for tangential component of magnetic field at S_1 and S_2, two equations are obtained for waves incident at each port, which are

$$\boldsymbol{a}_y \times \boldsymbol{H}_1^{inc} + \boldsymbol{a}_y \times \boldsymbol{H}_2^{inc} + \boldsymbol{a}_y \times \boldsymbol{H}_{1^+}^{(1)sct} = \boldsymbol{a}_y \times \boldsymbol{H}_{1^-}^{(3)sct} + \boldsymbol{a}_y \times \boldsymbol{H}_{2^+}^{(3)sct} \quad (1)$$

on S_1 and

$$\boldsymbol{a}_y \times \boldsymbol{H}_3^{inc} + \boldsymbol{a}_y \times \boldsymbol{H}_4^{inc} + \boldsymbol{a}_y \times \boldsymbol{H}_{2^-}^{(2)sct} = \boldsymbol{a}_y \times \boldsymbol{H}_{1^-}^{(3)sct} + \boldsymbol{a}_y \times \boldsymbol{H}_{2^+}^{(3)sct} \quad (2)$$

on S_2, where $\boldsymbol{H}_m^{inc}$ is the incident wave input from port m (m = 1, 2, 3, 4) and $\boldsymbol{H}_{i^\pm}^{(k)sct}$ is the scattering wave in region k (k = 1, 2, 3) generated by corresponding magnetic current at interface S_i (i = 1, 2). This latter magnetic field is represented by

$$\boldsymbol{H}_{i^\pm}^{(k)sct}(\boldsymbol{r}) = j\omega\varepsilon \iint_{S_i} \boldsymbol{G}_{\boldsymbol{m}k}(\boldsymbol{r} \mid \boldsymbol{r}') \cdot \boldsymbol{J}^{\pm}_{\mathrm{M}_i}(\boldsymbol{r}')\, dS_i' \,, \quad (3)$$

where $\boldsymbol{G}_{\boldsymbol{m}k}(\boldsymbol{r} \mid \boldsymbol{r}')$ is the magnetic dyadic Green's function of region k. $\boldsymbol{E}_{S_1}$ and $\boldsymbol{E}_{S_2}$ are the unknown quantities of (1) and (2), which will be approximated by trial functions.

Performing integration over S_1 after scalar multiplying $\boldsymbol{E}_{S_1}$ on both sides of (1), and similarly over S_2 after scalar multiplying $\boldsymbol{E}_{S_2}$ on both sides of (2), results in two equations containing vectors $\boldsymbol{H}_m^{inc}$ and $\boldsymbol{E}_{S_i}$, namely

$$N_{11} + N_{21} = -M_{11}^{(1)} - M_{11}^{(3)} + M_{21}^{(3)} \,, \quad (4)$$

and

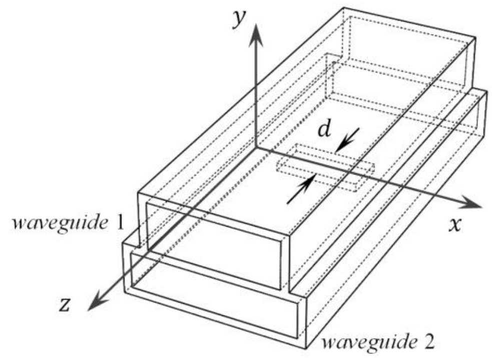

(a) Perspective view.

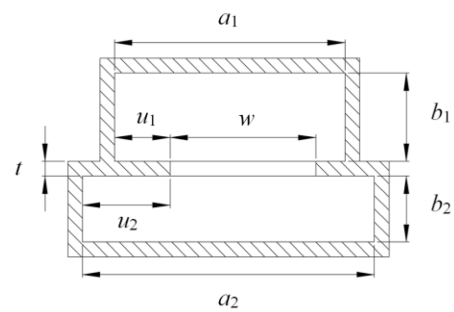

(b) Sectional view.

$$-N_{32} - N_{42} = -M_{22}^{(2)} - M_{22}^{(3)} + M_{12}^{(3)} \,, \quad (5)$$

where

$$N_{mi} = \iint_{S_i} \boldsymbol{H}_m^{inc}(\boldsymbol{r}) \cdot \left[\boldsymbol{a}_y \times \boldsymbol{E}_{S_i}(\boldsymbol{r})\right] dS_i \quad (6)$$

$$(m = 1,\ 2,\ 3,\ 4,\ i = 1,\ 2),$$

ar

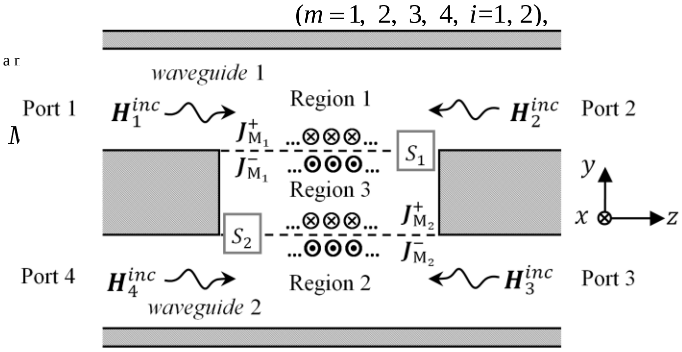

Fig. 2. Region division.

Combining (4) and (5), we obtain

$$
\begin{aligned}
& M_{11}^{(1)}+M_{11}^{(3)}-M_{21}^{(3)}+M_{22}^{(2)}+M_{22}^{(3)}-M_{12}^{(3)} \\
& =-\left(N_{11}+N_{21}-N_{32}-N_{42}\right) \\
& \triangleq S_{cp},
\end{aligned}
\tag{8}
$$

where S_{cp} denotes the compound scattering parameters of the coupling slot with arbitrary incident waves, which will be discussed later. According to (8), a general variational expression of stationary homogeneous form [14], [4] for S_{cp} is given by

$$
S_{cp}=\frac{\left(N_{11}+N_{21}-N_{32}-N_{42}\right)^2}{M_{11}^{(1)}+M_{11}^{(3)}+M_{22}^{(2)}+M_{22}^{(3)}-M_{21}^{(3)}-M_{12}^{(3)}}. \tag{9}
$$

It is shown in Appendix A that (9) is stationary with respect to small variations in $\boldsymbol{E}_{S_1}$ and $\boldsymbol{E}_{S_2}$. In this new expression, the effect of finite wall thickness is now included.

B. *Trial functions*

Before discussing the trial functions that could be suitable for (9), consider even mode and odd mode incident waves specified in Table I, for calculating different slot scattering parameters. We have used $\boldsymbol{H}_{10}^{(i)+}$ and $\boldsymbol{H}_{10}^{(i)-}$ to denote the normalized forward and backward traveling TE_{10} mode of waveguide i, i = 1, 2. Other scattering parameters can be obtained from those listed in Table I by employing symmetry and reciprocity of the structure, and are not considered here. Each mode consists of two or four symmetric incident waves input from different ports, resulting in symmetric and similar distribution of $\boldsymbol{E}_{S_1}$ and $\boldsymbol{E}_{S_2}$. For instance, when calculating S_{11} and S_{12}, such symmetry and similarity are shown in Fig. 3 and Fig. 4, where only the z-components of $\boldsymbol{E}_{S_1}$ and $\boldsymbol{E}_{S_2}$ are concerned because they are predominant in this situation. The results shown in Figs. 3 to 5 were obtained from HFSS, with the dimensions of the waveguides and the slot set as a_1 = a_2 = 15.8mm, b_1 = 6.0mm, b_2 = 3.0mm, w = 13.0mm, d = 5.0mm, t = 3.0mm and u_1 = u_2 = 1.4mm. The aspect ratio of the slot is 2.6. A negative magnitude corresponds to the electric field with an opposite direction. In Fig. 3 (a), the phase values around z = 0mm are not provided due to the instability of calculation when the corresponding magnitude is close to zero. For comparison, the results with a single incident wave input from Port 1 are also given in Fig. 5.

It is shown that the specified even mode and odd mode incident waves simplify the distribution of $\boldsymbol{E}_{S_1}$ and $\boldsymbol{E}_{S_2}$, and thus enable the trial functions to have similar and simple forms with only one expansion term, which should be sufficiently accurate even in case of a wide slot. Hence, appropriate trial functions are proposed as:

for even-modes,

TABLE I

SPECIFICATION OF EVEN MODE AND ODD MODE INCIDENT WAVES

Target		$\boldsymbol{H}_1^{inc}$	$\boldsymbol{H}_2^{inc}$	$\boldsymbol{H}_3^{inc}$	$\boldsymbol{H}_4^{inc}$	Complex Scale factor
S_{11} S_{12}	Even Mode	$\boldsymbol{H}_{10}^{(1)+}$	$\boldsymbol{H}_{10}^{(1)-}$	$\boldsymbol{0}$	$\boldsymbol{0}$	h_1^{e}
	Odd Mode	$\boldsymbol{H}_{10}^{(1)+}$	$-\boldsymbol{H}_{10}^{(1)-}$	$\boldsymbol{0}$	$\boldsymbol{0}$	h_1^{o}
S_{33} S_{34}	Even Mode	$\boldsymbol{0}$	$\boldsymbol{0}$	$\boldsymbol{H}_{10}^{(2)-}$	$\boldsymbol{H}_{10}^{(2)+}$	h_2^{e}
	Odd Mode	$\boldsymbol{0}$	$\boldsymbol{0}$	$\boldsymbol{H}_{10}^{(2)-}$	$-\boldsymbol{H}_{10}^{(2)+}$	h_2^{o}
S_{13} S_{14}	Even Mode	$\boldsymbol{H}_{10}^{(1)+}$	$\boldsymbol{H}_{10}^{(1)-}$	$\boldsymbol{H}_{10}^{(2)-}$	$\boldsymbol{H}_{10}^{(2)+}$	h_3^{e}
	Odd Mode	$\boldsymbol{H}_{10}^{(1)+}$	$-\boldsymbol{H}_{10}^{(1)-}$	$\boldsymbol{H}_{10}^{(2)-}$	$-\boldsymbol{H}_{10}^{(2)+}$	h_3^{o}

$$
\boldsymbol{E}_{S_1}=\boldsymbol{E}_S^{e}=\boldsymbol{a}_z\cdot A_i^{e}\cdot z\cdot\sin\frac{\pi\left(x-u_1\right)}{w}, \tag{10}
$$

$$
\boldsymbol{E}_{S_2}=h_i^{e}\cdot\boldsymbol{E}_S^{e}=\boldsymbol{a}_z\cdot A_i^{e}h_i^{e}\cdot z\cdot\sin\frac{\pi\left(x-u_1\right)}{w}, \tag{11}
$$

and for odd-modes,

$$
\boldsymbol{E}_{S_1}=\boldsymbol{E}_S^{o}=\boldsymbol{a}_z\cdot A_i^{o}\cdot\sin\frac{\pi\left(x-u_1\right)}{w}, \tag{12}
$$

$$
\boldsymbol{E}_{S_2}=h_i^{o}\cdot\boldsymbol{E}_S^{o}=\boldsymbol{a}_z\cdot A_i^{o}h_i^{o}\cdot\sin\frac{\pi\left(x-u_1\right)}{w}, \tag{13}
$$

where the superscript “e” and “o” represent even modes and odd modes respectively. A_i^{e} and A_i^{o} are arbitrary factors which will be eliminated in (9), i = 1, 2, 3. h_i^{e} and h_i^{o} are the complex scale factors between $\boldsymbol{E}_{S_1}$ and $\boldsymbol{E}_{S_2}$ corresponding to different modes specified in Table I, and this will be discussed in the next sub-section.

C. *Solutions of Slot Scattering Parameters*

1) *S_{11} and S_{12}*

Consider initially even mode incident waves for calculating S_{11} and S_{12} which are specified in Table I. Similarly, an additional superscript “e” is employed in certain symbols to denote the even modes. Substituting (10) and (11) into (9), and given that $\boldsymbol{H}_3^{inc}=\boldsymbol{H}_4^{inc}=\boldsymbol{0}$ which indicates that $N_{32}^{e}=N_{42}^{e}=0$, we obtain an expression of the compound scattering parameters with even modes, given as:

$$
\begin{aligned}
S_{cp1}^{e}=\left(N_{11}^{e}+N_{21}^{e}\right)^2\Big/\Big[& M_{11}^{(1)e}+M_{11}^{(3)e}+\left(h_1^{e}\right)^2\cdot M_{22}^{(2)e} \\
& +\left(h_1^{e}\right)^2\cdot M_{22}^{(3)e}-h_1^{e}M_{21}^{(3)e}-h_1^{e}\cdot M_{12}^{(3)e}\Big],
\end{aligned}
\tag{14}
$$

where

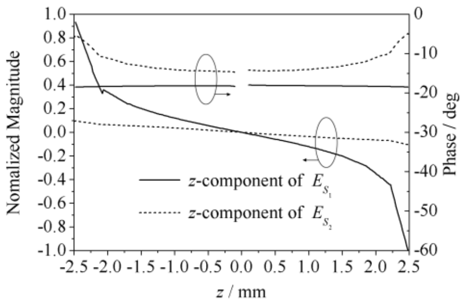

(a) Along z-axis at x = 10.9mm

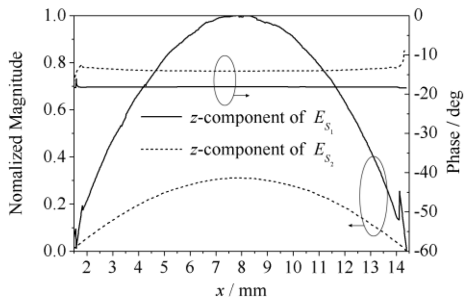

(b) Along x-axis at z = 1mm

Fig.3. z-component of $\boldsymbol{E}_{S_1}$ and $\boldsymbol{E}_{S_2}$ with even modes obtained from HFSS.

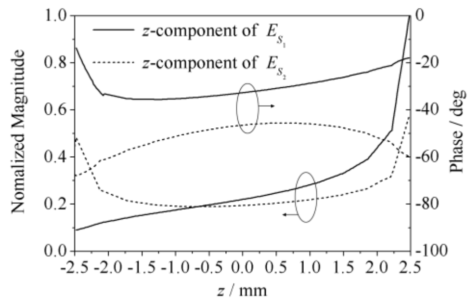

(a) Along z-axis at x = 10.9mm

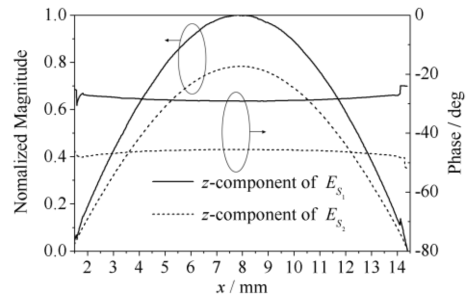

(b) Along x-axis at z = 1mm

Fig.5. z-component of $\boldsymbol{E}_{S_1}$ and $\boldsymbol{E}_{S_2}$ with single wave incidence input from Port 1 obtained from HFSS.

$$N_{11}^{\mathrm{e}} = \iint_{S_1} \boldsymbol{H}_{10}^{(1)+} \cdot \left[\boldsymbol{a}_y \times \boldsymbol{E}_S^{\mathrm{e}}\left(\boldsymbol{r}'\right)\right] dS_1 = 2\left(S_{11}+S_{12}-1\right) \quad (16\text{-a})$$

$$N_{21}^{\mathrm{e}} = \iint_{S_1} \boldsymbol{H}_{10}^{(1)-} \cdot \left[\boldsymbol{a}_y \times \boldsymbol{E}_S^{\mathrm{e}}\left(\boldsymbol{r}'\right)\right] dS_1 = 2\left(S_{11}+S_{12}-1\right) \quad (16\text{-b})$$

The right-hand sides of (16) are obtained according to usual mode analysis [15] as well as symmetry and reciprocity of the structure which indicate that $S_{11} = S_{22}$ and $S_{12} = S_{21}$. The scale factor h_1^{e} is obtained by minimizing (14). Expressions of N_{11}^{e}, N_{21}^{e}, $M_{ij}^{(k)\mathrm{e}}$ and h_1^{e} are listed in Appendix B. Given that $N_{32}^{\mathrm{e}} = N_{42}^{\mathrm{e}} = 0$, and combining (16) and (8), we obtain

$$S_{cp1}^{\mathrm{e}} = -\left(N_{11}^{\mathrm{e}} + N_{21}^{\mathrm{e}}\right) = -4\left(S_{11}+S_{12}-1\right). \quad (17)$$

We see that the compound scattering parameters, S_{cp1}^{e}, is a linear combination of S_{11} and S_{12}.

In the same way use is made of odd mode incident waves for calculating S_{11} and S_{12} as indicated in Table I. Similarly, an additional superscript "o" is employed in certain symbols. Substituting (12) and (13) into (9) gives the compound scattering parameters for odd modes as

$$S_{cp1}^{\mathrm{o}} = \left(N_{11}^{\mathrm{o}} + N_{21}^{\mathrm{o}}\right)^2 \Big/ \Big[M_{11}^{(1)\mathrm{o}} + M_{11}^{(3)\mathrm{o}} + \left(h_1^{\mathrm{o}}\right)^2 \cdot M_{22}^{(2)\mathrm{o}} + \left(h_1^{\mathrm{o}}\right)^2 \cdot M_{22}^{(3)\mathrm{o}} - h_1^{\mathrm{o}} M_{21}^{(3)\mathrm{o}} - h_1^{o} \cdot M_{12}^{(3)\mathrm{o}} \Big]. \quad (18)$$

$M_{ij}^{(k)\mathrm{e}}$ = (15)

$\cdot\left[\boldsymbol{a}_y\right.$ ... 3),

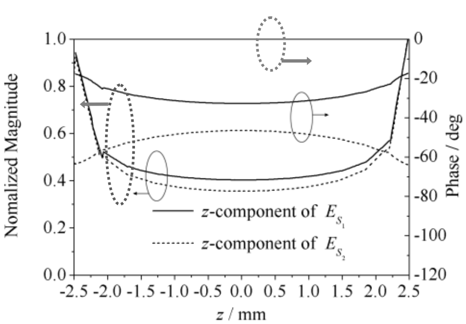

(a) Along z-axis at x = 10.9mm

and

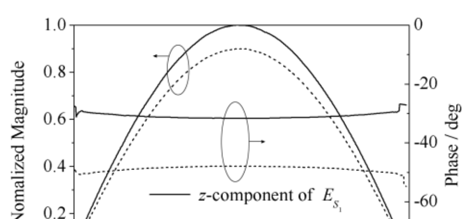

The scale factor h_1^{o} is obtained by minimizing (18) as described for the even modes. The corresponding result is

$$S_{cp1}^{\mathrm{o}} = -\left(N_{11}^{\mathrm{o}} + N_{21}^{\mathrm{o}}\right) = -4\left(S_{11} - S_{12} + 1\right). \tag{19}$$

The expressions of N_{11}^{o}, N_{21}^{o}, $M_{ij}^{(k)\mathrm{o}}$ and h_1^{o} are also listed in Appendix B.

Combining (17) and (19), S_{11} and S_{12} are expressed as

$$S_{11} = -\frac{S_{cp1}^{\mathrm{o}} + S_{cp1}^{\mathrm{e}}}{8}, \tag{20}$$

$$S_{12} = \frac{S_{cp1}^{\mathrm{o}} - S_{cp1}^{\mathrm{e}}}{8} + 1, \tag{21}$$

where S_{cp1}^{e} and S_{cp1}^{o} are obtained from (14) and (18), respectively.

2) S_{33} and S_{34}

In the same way, we obtain

$$S_{cp2}^{\mathrm{e}} = \left(h_2^{\mathrm{e}}\right)^2 \cdot \left(N_{32}^{\mathrm{e}} + N_{42}^{\mathrm{e}}\right)^2 \Big/ \Big[M_{11}^{(1)\mathrm{e}} + M_{11}^{(3)\mathrm{e}} + \left(h_2^{\mathrm{e}}\right)^2 \cdot M_{22}^{(2)\mathrm{e}} + \left(h_2^{\mathrm{e}}\right)^2 \cdot M_{22}^{(3)\mathrm{e}} - h_2^{\mathrm{e}} M_{21}^{(3)\mathrm{e}} - h_2^{\mathrm{e}} \cdot M_{12}^{(3)\mathrm{e}}\Big], \tag{22}$$

$$S_{cp2}^{\mathrm{o}} = \left(h_2^{\mathrm{o}}\right)^2 \cdot \left(N_{32}^{\mathrm{o}} + N_{42}^{\mathrm{o}}\right)^2 \Big/ \Big[M_{11}^{(1)\mathrm{o}} + M_{11}^{(3)\mathrm{o}} + \left(h_2^{\mathrm{o}}\right)^2 \cdot M_{22}^{(2)\mathrm{o}} + \left(h_2^{\mathrm{o}}\right)^2 \cdot M_{22}^{(3)\mathrm{o}} - h_2^{\mathrm{o}} M_{21}^{(3)\mathrm{o}} - h_2^{\mathrm{o}} \cdot M_{12}^{(3)\mathrm{o}}\Big], \tag{23}$$

where the incident waves are chosen as shown in Table I. The scale factors h_2^{e} and h_2^{o} are obtained by minimizing (22) and (23). The expressions of N_{32}^{e}, N_{42}^{e}, h_2^{e}, N_{32}^{o}, N_{42}^{o} and h_2^{o} are listed in Appendix B. It can be shown that

$$S_{cp2}^{\mathrm{e}} = h_2^{\mathrm{e}} N_{32}^{\mathrm{e}} + h_2^{\mathrm{e}} N_{42}^{\mathrm{e}} = -4\left(S_{33} + S_{34} - 1\right), \tag{24}$$

$$S_{cp2}^{\mathrm{o}} = h_2^{\mathrm{o}} N_{32}^{\mathrm{o}} + h_2^{\mathrm{o}} N_{42}^{\mathrm{o}} = -4\left(S_{33} - S_{34} + 1\right). \tag{25}$$

Combining (24) and (25), S_{33} and S_{34} can be expressed as

$$S_{33} = -\frac{S_{cp2}^{\mathrm{o}} + S_{cp2}^{\mathrm{e}}}{8}, \tag{26}$$

$$S_{34} = \frac{S_{cp2}^{\mathrm{o}} - S_{cp2}^{\mathrm{e}}}{8} + 1. \tag{27}$$

3) S_{13} and S_{14}

Similarly, we obtain

$$S_{cp3}^{\mathrm{e}} = \left[N_{11}^{\mathrm{e}} + N_{21}^{\mathrm{e}} - h_3^{\mathrm{e}}\left(N_{32}^{\mathrm{e}} + N_{42}^{\mathrm{e}}\right)\right]^2 \Big/ \Big[M_{11}^{(1)\mathrm{e}} + M_{11}^{(3)\mathrm{e}} + \left(h_3^{\mathrm{e}}\right)^2 \cdot M_{22}^{(2)\mathrm{e}} + \left(h_3^{\mathrm{e}}\right)^2 \cdot M_{22}^{(3)\mathrm{e}} - h_3^{\mathrm{e}} \cdot M_{21}^{(3)\mathrm{e}} - h_3^{\mathrm{e}} \cdot M_{12}^{(3)\mathrm{e}}\Big], \tag{28}$$

$$S_{cp3}^{\mathrm{o}} = \left[N_{11}^{\mathrm{o}} + N_{21}^{\mathrm{o}} - h_3^{\mathrm{o}}\left(N_{32}^{\mathrm{o}} + N_{42}^{\mathrm{o}}\right)\right]^2 \Big/ \Big[M_{11}^{(1)\mathrm{o}} + M_{11}^{(3)\mathrm{o}} + \left(h_3^{\mathrm{o}}\right)^2 \cdot M_{22}^{(2)\mathrm{o}} + \left(h_3^{\mathrm{o}}\right)^2 \cdot M_{22}^{(3)\mathrm{o}} - h_3^{\mathrm{o}} \cdot M_{21}^{(3)\mathrm{o}} - h_3^{\mathrm{o}} \cdot M_{12}^{(3)\mathrm{o}}\Big], \tag{29}$$

where the incident waves are chosen as shown in Table I. The scale factors h_3^{e} and h_3^{o} are obtained by minimizing (28) and (29), and the results are given in Appendix B. In this case we obtain

$$S_{cp3}^{\mathrm{e}} = -\left(N_{11}^{\mathrm{e}} + N_{21}^{\mathrm{e}} - h_3^{\mathrm{e}} N_{32}^{\mathrm{e}} - h_3^{\mathrm{e}} N_{42}^{\mathrm{e}}\right) = -4\left(S_{11} + S_{12} - 1\right) - 4\left(S_{33} + S_{34} - 1\right) - 8\left(S_{13} + S_{14}\right), \tag{30}$$

$$S_{cp3}^{\mathrm{o}} = -\left(N_{11}^{\mathrm{o}} + N_{21}^{\mathrm{o}} - h_3^{\mathrm{o}} N_{32}^{\mathrm{o}} - h_3^{\mathrm{o}} N_{42}^{\mathrm{o}}\right) = -4\left(S_{11} - S_{12} + 1\right) - 4\left(S_{33} - S_{34} + 1\right) - 8\left(S_{13} - S_{14}\right). \tag{31}$$

Combining (17), (19), (24), (25), (30) and (31), S_{13} and S_{14} can be expressed as

$$S_{13} = \frac{\left(S_{cp1}^{\mathrm{o}} + S_{cp1}^{\mathrm{e}}\right) + \left(S_{cp2}^{\mathrm{o}} + S_{cp2}^{\mathrm{e}}\right) - \left(S_{cp3}^{\mathrm{o}} + S_{cp3}^{\mathrm{e}}\right)}{16}, \tag{32}$$

$$S_{14} = \frac{\left(S_{cp3}^{\mathrm{o}} - S_{cp3}^{\mathrm{e}}\right) - \left(S_{cp1}^{\mathrm{o}} - S_{cp1}^{\mathrm{e}}\right) - \left(S_{cp2}^{\mathrm{o}} - S_{cp2}^{\mathrm{e}}\right)}{16}. \tag{33}$$

III. RESULTS

A Matlab code was developed for the new formulation and results obtained were compared with values calculated by the Ansoft HFSS v10 software package. Fig. 6 shows the calculated results of S_{11}, S_{12}, S_{13} and S_{14} for a coupling slot with an aspect ratio of 2.6, which was previously discussed in Section II *B*, for the frequency range 12 to 18GHz. Results obtained from the new formulation are in excellent agreement with HFSS where the error is within about ±0.2 dB and ±2degrees for all scattering parameters as shown in Fig. 6. The error is seen to increase to around 0.3 dB and 6 degrees for S_{11} at the lowest frequencies in the band.

In Fig. 7 results are given for another slot with an aspect ratio of 2, this time in X band. Although S_{12} has a magnitude error up to 0.3dB, S_{11}, S_{13}, and S_{14} are of acceptable accuracy and the overall errors is within ±0.1 dB and ±3degrees. Characteristics of the error of S_{33} and S_{34} are similar to those of S_{11} and S_{12}.

In Table II we compare the computation times of the two methods for obtaining the results shown in Fig. 6. The operating computer has a dual-core CPU running at 2.80GHz and a RAM

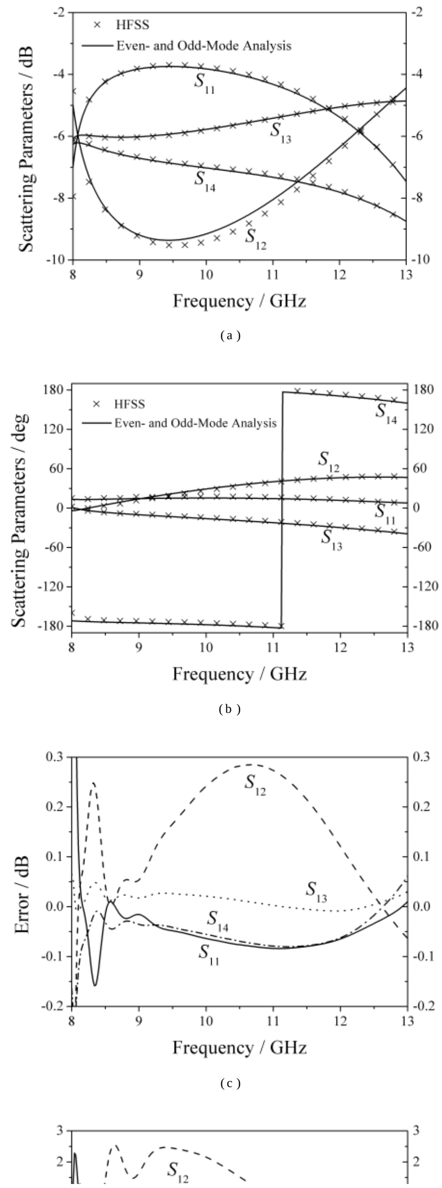

F

P

1

2

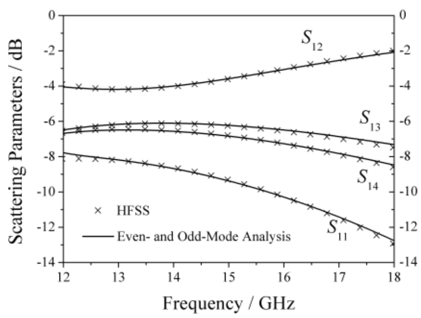

(a)

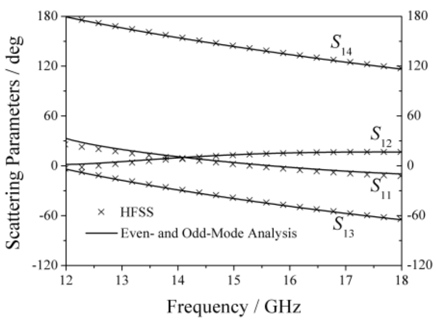

(b)

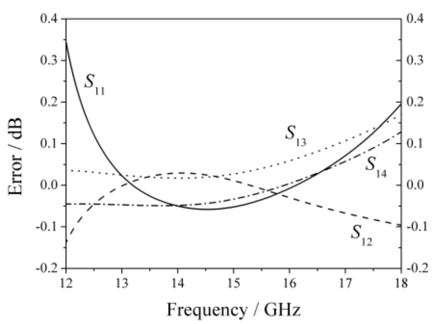

(c)

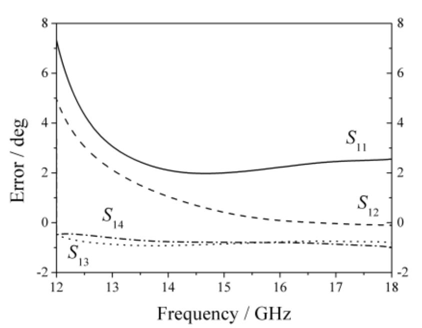

(d)

Fig. 6. Scattering parameters of a coupling slot at Ku band. (a) Magnitude. (b) Phase. (c) Error in magnitude. (d) Error in phase. The dimensions are a_1 = a_2 = 15.8mm, b_1 = 6.0mm, b_2 = 3.0mm, w = 13.0mm, d = 5.0mm, t = 3.0mm and u_1 = u_2 = 1.4mm.

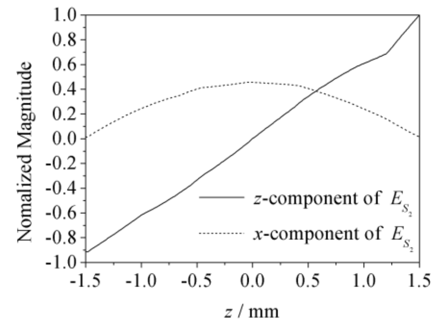

(a) Along z-axis at x = 10.9mm

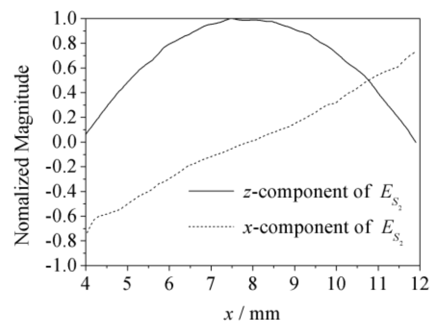

(b) Along x-axis at z = 0.5mm

Fig. 8. Normalized magnitude of z- and x-component of $\boldsymbol{E}_{S_2}$ with even modes obtained from HFSS. The dimensions are a_1 = a_2 = 15.8mm, b_1 = 6.0mm, b_2 = 3.0mm, w = 8.0mm, d = 3.0mm, t = 3.0mm and u_1 = u_2 = 3.9mm.

of 4GB. Since the Matlab code was not developed for parallel processing purpose, only one processor was used during the computation. However, the new formulation is still much faster than HFSS with 2 processors employed, saving over 99% of the computation time.

IV. Discussion

It is found that for a relatively short slot in terms of wavelength, accurate results for S_{cp}^{e} may not be achievable. The reason is because in the simplification of the trial functions the x-component of $\boldsymbol{E}_S^{\mathrm{e}}$ is ignored. For a short slot with w = 8.0mm (0.38 λ_0 at center frequency of 14.25GHz, where λ_0 denotes the wavelength in open space), the normalized magnitudes of z- and x-component of $\boldsymbol{E}_{S_2}$ with even mode incident waves are given in Fig. 8. In this situation, it is shown that the x-component has become significant, which also occurs when considering $\boldsymbol{E}_{S_1}$. It is believed that the method would provide better results if more appropriate trial functions were employed for even modes, such as

$$\boldsymbol{E}_{S_1} = \boldsymbol{E}_S^{\mathrm{e}} = A_i^{\mathrm{e}} \cdot \left[\boldsymbol{a}_z \cdot z \cdot \sin\frac{\pi\left(x-u_1\right)}{w} + \boldsymbol{a}_x \cdot B_i^{\mathrm{e}} \cdot \left(x-u_1-\frac{w}{2}\right)\cdot\cos\frac{\pi z}{d}\right], \tag{34}$$

$$\boldsymbol{E}_{S_2} = h_i^{\mathrm{e}} \cdot \boldsymbol{E}_S^{\mathrm{e}'} = h_i^{\mathrm{e}} \cdot A_i^{\mathrm{e}} \cdot \left[\boldsymbol{a}_z \cdot z \cdot \sin\frac{\pi\left(x-u_1\right)}{w} + \boldsymbol{a}_x \cdot C_i^{\mathrm{e}} \cdot \left(x-u_1-\frac{w}{2}\right)\cdot\cos\frac{\pi z}{d}\right], \tag{35}$$

where B_i^{e} and C_i^{e} are complex scale factors obtained by minimizing the corresponding variational expression of S_{cp}^{e}. However, introducing the *x*-component in trial functions will significantly complicate the solution and thus is not considered further here. With the presently chosen simple shape function there is a restriction on the slot length, which is

$$w \geq \lambda_0 / 2. \tag{36}$$

In addition, for best accuracy, the slot aspect ratio is recommended to be greater than 2.5.

It is shown that the new formulation demonstrates much shorter computation time compared to HFSS, and it can be easily sped up through parallel computing since the calculation of each term in the summation is independent. With shorter computation time, the new formulation is useful for large scale problems that may require adaptive optimization, especially when employing equivalent circuit analysis for complicate waveguide components that contain slots. The formulation can be used for fast extraction of the equivalent circuit parameters of a slot, as the dimensions change during the adaptive process.

V. Conclusion

Based on a new variational method, an even- and odd-mode analysis of broadwall coupling slot between waveguides is proposed, which is capable of dealing with the effect of finite wall thickness. A variational expression of compound scattering parameters is first derived, and simple trial functions are then determined from specified even-mode and odd-mode incident waves. Each mode consists of two or four symmetric incident waves, enabling the adoption of one-expansion-term trial functions with sufficient accuracy even in the instance of wide slots. With the variational expression and corresponding trial functions, compound scattering parameters with respect to even mode and odd mode incident waves are acquired. Combining the results, analytical solutions of the slot scattering parameters are achieved, which are valuable for practical design and optimization. Calculated results demonstrate excellent agreement with those of HFSS, with errors within ±0.2 dB and ±3degrees. The computation time is, however, significantly shorter than with HFSS. A restriction is proposed as $w \geq \lambda_0 / 2$ to achieve such accuracy. The aspect ratio of slots can be as small as 2, but it is recommended to be greater than 2.5. It is believed that by employing more appropriate trial functions with corresponding simplification of the formulas may help to solve the limitation of short slots (in terms of wavelength), which could be followed up as a refinement of the method.

Appendix A

In this Appendix we demonstrate the stationary nature of the variational functional (9). Taking the first variation on both sides of (9) with respect to $\boldsymbol{E}_{S_1}$, we have

$$\begin{aligned}\delta S_{cp}\left[\boldsymbol{E}_{S_1}\right] = \Big\{ & 2\left(N_{11}+N_{21}-N_{32}-N_{42}\right) \\ & \cdot\left(\delta N_{11}+\delta N_{21}-\delta N_{32}-\delta N_{42}\right) \\ & \cdot\left[M_{11}^{(1)}+M_{11}^{(3)}+M_{22}^{(2)}+M_{22}^{(3)}-M_{21}^{(3)}-M_{12}^{(3)}\right] \\ & -\left(N_{11}+N_{21}-N_{32}-N_{42}\right)^2 \\ & \cdot\delta M_{11}^{(1)}+\delta M_{11}^{(3)}+\delta M_{22}^{(2)}+\delta M_{22}^{(3)}-\delta M_{21}^{(3)}-\delta M_{12}^{(3)}\Big\} \\ & \Big/\left[M_{11}^{(1)}+M_{11}^{(3)}+M_{22}^{(2)}+M_{22}^{(3)}-M_{21}^{(3)}-M_{12}^{(3)}\right]^2.\end{aligned} \tag{37}$$

According to (8), (37) can be simplified as

$$\begin{aligned}\delta S_{cp}\left[\boldsymbol{E}_{S_1}\right] = & -2\cdot\left(\delta N_{11}+\delta N_{21}-\delta N_{32}-\delta N_{42}\right) \\ & -\left[\delta M_{11}^{(1)}+\delta M_{11}^{(3)}+\delta M_{22}^{(2)}+\delta M_{22}^{(3)}-\delta M_{21}^{(3)}-\delta M_{12}^{(3)}\right].\end{aligned} \tag{38}$$

It is easy to find that

$$\delta N_{m1} = \iint_{S_1} \boldsymbol{H}_m^{inc}\left(\boldsymbol{r}\right)\cdot\left[\boldsymbol{a}_y \times \delta\boldsymbol{E}_{S_1}\left(\boldsymbol{r}\right)\right] dS_1 \quad (m=1,\ 2), \tag{39}$$

$$\delta N_{m2} = 0 \quad (m=3,\ 4), \tag{40}$$

$$\begin{aligned}\delta M_{11}^{(k)} = 2j\omega\varepsilon \iint_{S_1}\iint_{S_1} & \left[\boldsymbol{a}_y \times \delta\boldsymbol{E}_{S_1}\left(\boldsymbol{r}\right)\right]\cdot\boldsymbol{G}_{\boldsymbol{m}k}\left(\boldsymbol{r}\,|\,\boldsymbol{r}'\right) \\ & \cdot\left[\boldsymbol{a}_y \times \boldsymbol{E}_{S_1}\left(\boldsymbol{r}'\right)\right] dS_1' dS_1 \ (k=1, 3),\end{aligned} \tag{41}$$

$$\delta M_{22}^{(k)} = 0 \quad (k=2, 3), \tag{42}$$

and

$$\begin{aligned}\delta M_{12}^{(3)} = \delta M_{21}^{(3)} = j\omega\varepsilon \iint_{S_1}\iint_{S_2} & \left[\boldsymbol{a}_y \times \delta\boldsymbol{E}_{S_1}\left(\boldsymbol{r}\right)\right] \\ & \cdot\boldsymbol{G}_{\boldsymbol{m}3}\left(\boldsymbol{r}\,|\,\boldsymbol{r}'\right)\cdot\left[\boldsymbol{a}_y \times \boldsymbol{E}_{S_2}\left(\boldsymbol{r}'\right)\right] dS_2' dS_1.\end{aligned} \tag{43}$$

Substituting (39) ~ (43) into (38), we obtain

$$\delta S_{cp}\left[\boldsymbol{E}_{S_1}\right]=2\iint_{S_1}\delta\boldsymbol{E}_{S_1}(\boldsymbol{r})\cdot\Big\{\boldsymbol{a}_y\times\boldsymbol{H}_1^{inc}(\boldsymbol{r})+\boldsymbol{a}_y\times\boldsymbol{H}_2^{inc}(\boldsymbol{r})+ j\omega\varepsilon\cdot\boldsymbol{a}_y\times\iint_{S_1}\left[\boldsymbol{G}_{m1}\left(\boldsymbol{r}\,|\,\boldsymbol{r}'\right)+\boldsymbol{G}_{m3}\left(\boldsymbol{r}\,|\,\boldsymbol{r}'\right)\right]\cdot\left[\boldsymbol{a}_y\times\boldsymbol{E}_{S_1}\left(\boldsymbol{r}'\right)\right]dS_1' -j\omega\varepsilon\cdot\boldsymbol{a}_y\times\iint_{S_2}\boldsymbol{G}_{m3}\left(\boldsymbol{r}\,|\,\boldsymbol{r}'\right)\cdot\left[\boldsymbol{a}_y\times\boldsymbol{E}_{S_2}\left(\boldsymbol{r}'\right)\right]dS_2'\Big\}dS_1. \quad (44)$$

According to (1) and (3), (44) finally becomes

$$\delta S_{cp}\left[\boldsymbol{E}_{S_1}\right]=0\,. \quad (45)$$

In the same way, it can be found that

$$\delta S_{cp}\left[\boldsymbol{E}_{S_2}\right]=0\,. \quad (46)$$

Equation (45) and (46) indicate that (9) satisfies stationary properties with respect to small variations in $\boldsymbol{E}_{S_1}$ and $\boldsymbol{E}_{S_2}$.

Appendix B

Listed here are the useful expressions obtained from the proposed even and odd modes trial functions.

Even modes:

$$N_{11}^{\mathrm{e}}=N_{21}^{\mathrm{e}}=-F_1\cdot G_1\left(a_1,u_1\right)\cdot D_{\mathrm{e}}\left(k_{10}^{(1)}\right) \quad (47)$$

$$N_{32}^{\mathrm{e}}=N_{42}^{\mathrm{e}}=-F_2\cdot G_1\left(a_2,u_2\right)\cdot D_{\mathrm{e}}\left(k_{10}^{(2)}\right) \quad (48)$$

$$M_{11}^{(1)\mathrm{e}}=j\omega\varepsilon\sum_{m=1}^{\infty}\sum_{n=0}^{\infty}\frac{\delta_n}{a_1b_1\left[k_{mn}^{(1)}\right]^2}\left[1-\frac{1}{k^2}\left(\frac{m\pi}{a_1}\right)^2\right]\cdot\left[G_m\left(a_1,u_1\right)\right]^2\cdot H_{\mathrm{e}}\left(k_{mn}^{(1)}\right) \quad (49)$$

$$M_{22}^{(2)\mathrm{e}}=j\omega\varepsilon\sum_{m=1}^{\infty}\sum_{n=0}^{\infty}\frac{\delta_n}{a_2b_2\left[k_{mn}^{(2)}\right]^2}\left[1-\frac{1}{k^2}\left(\frac{m\pi}{a_2}\right)^2\right]\cdot\left[G_m\left(a_2,u_2\right)\right]^2\cdot H_{\mathrm{e}}\left(k_{mn}^{(2)}\right) \quad (50)$$

$$M_{11}^{(3)\mathrm{e}}=M_{22}^{(3)\mathrm{e}}=j\omega\varepsilon\sum_{n=0}^{\infty}\frac{w\delta_n}{2t\left[k_{1n}^{(3)}\right]^2}\left[1-\frac{1}{k^2}\left(\frac{\pi}{w}\right)^2\right]\cdot\left\{\frac{d^3}{12}+\frac{1}{k_{1n}^{(3)}}\cdot\left[d-\frac{2}{k_{1n}^{(3)}}\tan\left(\frac{k_{1n}^{(3)}d}{2}\right)\right]\right\} \quad (51)$$

$$M_{21}^{(3)\mathrm{e}}=M_{12}^{(3)\mathrm{e}}=j\omega\varepsilon\sum_{n=0}^{\infty}\frac{(-1)^n\,w\delta_n}{2t\left[k_{1n}^{(3)}\right]^2}\left[1-\frac{1}{k^2}\left(\frac{\pi}{w}\right)^2\right]\cdot\left\{\frac{d^3}{12}+\frac{1}{k_{1n}^{(3)}}\cdot\left[d-\frac{2}{k_{1n}^{(3)}}\tan\left(\frac{k_{1n}^{(3)}d}{2}\right)\right]\right\} \quad (52)$$

$$h_1^{\mathrm{e}}=\frac{M_{12}^{(3)\mathrm{e}}}{M_{22}^{(2)\mathrm{e}}+M_{22}^{(3)\mathrm{e}}} \quad (53)$$

$$h_2^{\mathrm{e}}=\frac{M_{11}^{(1)\mathrm{e}}+M_{11}^{(3)\mathrm{e}}}{M_{12}^{(3)\mathrm{e}}} \quad (54)$$

$$h_3^{\mathrm{e}}=\frac{N_{32}^{\mathrm{e}}\cdot\left[M_{11}^{(1)\mathrm{e}}+M_{11}^{(3)\mathrm{e}}\right]-N_{11}^{\mathrm{e}}\cdot M_{12}^{(3)\mathrm{e}}}{N_{32}^{\mathrm{e}}\cdot M_{12}^{(3)\mathrm{e}}-N_{11}^{\mathrm{e}}\cdot\left[M_{22}^{(2)\mathrm{e}}+M_{22}^{(3)\mathrm{e}}\right]} \quad (55)$$

Odd Modes:

$$N_{11}^{\mathrm{o}}=N_{21}^{\mathrm{o}}=2jF_1\cdot G_1\left(a_1,u_1\right)\cdot\sin\left(k_{10}^{(1)}d/2\right) \quad (56)$$

$$N_{32}^{\mathrm{o}}=N_{42}^{\mathrm{o}}=-2jF_2\cdot G_2\left(a_2,u_2\right)\cdot\sin\left(k_{10}^{(2)}d/2\right) \quad (57)$$

$$M_{11}^{(1)\mathrm{o}}=j\omega\varepsilon\sum_{m=1}^{\infty}\sum_{n=0}^{\infty}\frac{2\delta_n}{a_1b_1\left[k_{mn}^{(1)}\right]^2}\left[1-\frac{1}{k^2}\left(\frac{m\pi}{a_1}\right)^2\right]\cdot\left[G_m\left(a_1,u_1\right)\right]^2\cdot H_{\mathrm{o}}\left(k_{mn}^{(1)}\right) \quad (58)$$

$$M_{22}^{(2)\mathrm{o}}=j\omega\varepsilon\sum_{m=1}^{\infty}\sum_{n=0}^{\infty}\frac{2\delta_n}{a_2b_2\left[k_{mn}^{(2)}\right]^2}\left[1-\frac{1}{k^2}\left(\frac{m\pi}{a_2}\right)^2\right]\cdot\left[G_m\left(a_2,u_2\right)\right]^2\cdot H_{\mathrm{o}}\left(k_{mn}^{(2)}\right) \quad (59)$$

$$M_{11}^{(3)\mathrm{o}}=M_{22}^{(3)\mathrm{o}}=j\omega\varepsilon\sum_{n=0}^{\infty}\frac{wd\delta_n}{2t\left[k_{1n}^{(3)}\right]^2}\left[1-\frac{1}{k^2}\left(\frac{\pi}{w}\right)^2\right] \quad (60)$$

$$M_{21}^{(3)\mathrm{o}}=M_{12}^{(3)\mathrm{o}}=j\omega\varepsilon\sum_{n=0}^{\infty}\frac{(-1)^n\,wd\delta_n}{2t\left[k_{1n}^{(3)}\right]^2}\left[1-\frac{1}{k^2}\left(\frac{\pi}{w}\right)^2\right] \quad (61)$$

$$h_1^{o} = \frac{M_{12}^{(3)o}}{M_{22}^{(2)o} + M_{22}^{(3)o}} \tag{62}$$

$$h_2^{o} = \frac{M_{11}^{(1)o} + M_{11}^{(3)o}}{M_{12}^{(3)o}} \tag{63}$$

$$h_3^{o} = \frac{N_{32}^{o} \cdot \left[M_{11}^{(1)o} + M_{11}^{(3)o} \right] - N_{11}^{o} \cdot M_{12}^{(3)o}}{N_{32}^{e} \cdot M_{12}^{(3)o} - N_{11}^{o} \cdot \left[M_{22}^{(2)o} + M_{22}^{(3)o} \right]} \tag{64}$$

In the above expressions,

$$G_m\left(a,u\right) = \frac{a^2 w}{\pi\left(a^2 - w^2 m^2\right)} \cdot \left[\sin\frac{m\pi\left(w+u\right)}{a} + \sin\frac{m\pi u}{a} \right] \tag{65}$$

$$D_e\left(\beta\right) = \left[d\cos\left(\frac{\beta d}{2}\right) - \frac{2}{\beta}\sin\left(\frac{\beta d}{2}\right) \right] \tag{66}$$

$$H_e\left(\beta\right) = \frac{d^3}{6} + \frac{2j}{\beta} e^{-j\beta d/2} \left(\frac{d}{2} + \frac{1}{j\beta}\right) \cdot \left[d\cos\left(\frac{\beta d}{2}\right) - \frac{2}{\beta}\sin\left(\frac{\beta d}{2}\right) \right] \tag{67}$$

$$H_o\left(\beta\right) = d - \frac{2}{\beta}\sin\left(\frac{\beta d}{2}\right) e^{-j\beta d/2} \tag{68}$$

$$\delta_n = \begin{cases} 1, & n = 0 \\ 2, & n > 0 \end{cases} \tag{69}$$

$$F_i = j\sqrt{\frac{2}{a_i b_i k_{10}^{(i)} k\eta}} \tag{70}$$

$$k_{mn}^{(i)} = \sqrt{k^2 - \left(\frac{m\pi}{a_i}\right)^2 - \left(\frac{n\pi}{b_i}\right)^2} \quad i = 1,\ 2 \tag{71}$$

$$k_{1n}^{(3)} = \sqrt{k^2 - \left(\frac{\pi}{w}\right)^2 - \left(\frac{n\pi}{t}\right)^2} \tag{72}$$

ω is the angular frequency, ε is the permittivity, k is the wave number and η is the wave impedance.

References

[1] A. F. Stevenson, "Theory of slots in rectangular wave-guides", *J. Appl. Phys.*, vol. 19, pp. 24–38, Jan. 1948.

[2] L. Lewin, "Some observations on waveguide coupling through medium-sized slots", *Proc. IEE, Pt. C*, Vol.107, pp. 171-178, 1960

[3] V. M. Pandharipande, B. N. Das, "Coupling of Waveguides through Large Apertures", *IEEE Trans. Microwave Theory Tech.*, Vol. 26, pp. 209-212, Mar. 1978.

[4] A. J. Sangster, "Variational method for the analysis of waveguide coupling", *Proceedings of the Institution of Electrical Engineers*, Vol. 112, pp. 2171-2179, 1965.

[5] S. R. Rengarajan, "Characteristics of a longitudinal/transverse coupling slot in crossed rectangular waveguides," *IEEE Trans. Microwave Theory Tech.*, vol. 37, pp. 1171–1177, Aug. 1989.

[6] H.-Y. Yee, "Slotted waveguide directional coupler characteristics", *IEEE Trans. Microwave Theory Tech.*, Vol.38, pp. 1497 – 1502, Oct. 1990.

[7] A. J. Sangster, Hanyang Wang, "A Generalized Analysis for a Class of Rectangular Waveguide Coupler Employing Narrow Wall Slots", *IEEE Trans. Microwave Theory Tech.*, Vol.44, pp. 283-290, Feb. 1996.

[8] Wu Ren, Ben-Qing Gao, Zheng-Hui Xue, et al, "Full-wave analysis of broad wall slot's Characteristics in rectangular waveguides", *IEEE Trans. Antennas Propagat.*, vol. 52, pp. 2436-2444, Sep. 2004.

[9] Kantartzis, Nikolaos V. Tsiboukis, Theodoros D., "Higher Order FDTD Schemes for Waveguide and Antenna Structures", *Synthesis Lectures on Computational Electromagnetics*, Morgan & Claypool, 2006, Chapter 7.

[10] J.K. Park, S.W. Nam, "A general rigorous analysis of arbitrary-shaped multiaperture-coupled directional coupler between two dissimilar rectangular waveguides crossing with an arbitrary angle", *Microw. Opt. Technol. Lett.*, Vol. 18, pp. 43–46, May. 1998.

[11] T. Sieverding, U. Papziner, F. Arndt, "Mode-matching CAD of rectangular or circular multiaperture narrow-wall couplers", *IEEE Trans. Microwave Theory Tech.*, Vol. 45, pp. 1034-1040, Jul. 1997.

[12] Jiang, Z. Shen, Z. "Mode-matching analysis of large aperture coupling and its applications to the design of waveguide directional couplers", *IEE Proceedings - Microwaves Antennas and Propagation*, Vol.150, Iss.6, pp.422-428, 2003.

[13] Fahmi, M. M., Ruiz-Cruz, J. A. and Zaki, K. A., "E and H-plane wide-band ridge waveguide couplers". *International Journal of RF and Microwave Computer-Aided Engineering*, Vol. 18, Iss. 4, pp:348–358, 2008.

[14] H. Levine, J. Schwinger, "On the theory of electromagnetic wave diffraction by an aperture in an infinite plane conducting screen", *Communications on Pure and Applied Mathematics*, Vol. 3, Issue 4, pp. 355–391, Dec. 1950.

[15] R. E. Collin, *Field theory of guided waves*, Wiley-IEEE Press, 1991, Chapter 7.

Wang Wenzhi received the B.S. degree in information engineering, M. S. degree in electromagnetic and microwave technology from Shanghai Jiao Tong University, Shanghai, China, in 2009 and 2011, respectively, where he is currently working towards the Ph.D. degree.

His research interests include microwave antennas, phased arrays, calibration techniques for arrays, guided wave theory and waveguide components.

Ye Sheng was born in Guangdong Province, China, in Oct. 1983. He received the B.S. degree in information engineering from South China University of Technology, Guangzhou, China, in 2006, and M.S. degree in electromagnetic and microwave technology from Shanghai Jiao Tong University, Shanghai, China, in 2009, where he is currently working towards the Ph.D. degree.

His main research interests are in high gain planar antennas for wireless communications, especially high efficiency array antenna for mobile satellite communication.

Liang Xianling (M'11) received the B.Sc. degree in electronic engineering from Xi'dian University, Xi'an, China, in 2002, and the Ph.D. degree in electric

engineering from Shanghai University, Shanghai, China, in 2007.

From 2007 to 2008, he was a Postdoctoral Research Fellow with the Institut National de la Recherche Scientifique (INRS), Université du Quebec, Montréal, QC, Canada. In December 2008, he joined the Department of Electronic Engineering, Shanghai Jiao Tong University, as a Lecturer. He has authored or coauthored over 80 papers in refereed journals and conference proceedings. His current research interests include microwave and millimeter-wave antennas, integrated antennas, wideband and active antennas, phased arrays.

Dr. Liang was the recipient of the Award of Shanghai Municipal Excellent Doctoral Dissertation in 2008, the Nomination of National Excellent Doctoral Dissertation in 2009, and the Best Paper Award presented at the 2010 International Workshop on Antenna Technology: Small Antennas, Innovative Structures, and Materials.

Jin Ronghong (M'09) received the B.S. degree in electronic engineering, M.S. degree in electromagnetic and microwave technology, and Ph.D. degree in communication and electronic systems from Shanghai Jiao Tong University, Shanghai, China, in 1983, 1986, and 1993, respectively.

In 1986, he joined the Faculty of the Department of Electronic Engineering, Shanghai Jiao Tong University, where he has been an Assistant, a Lecturer, an Associate Professor, and currently, a Professor. From 1997 to 1999, he was a Visiting Scholar with the Department of Electrical and Electronic Engineering, Tokyo Institute of Technology. He has authored or coauthored over 200 papers in refereed journals and conference proceedings and coauthored one book. His main areas of research interest are antennas, electromagnetic theory, numerical techniques of solving field problems, and interconnects and packages of high-speed integrated circuits (ICs).

Dr. Jin is a Senior Member of the Chinese Institute of Electronics. He was the recipient of a Shanghai Science and Technology Progress Award.

Trevor S. Bird (S'71–M'76–SM'85–F'97) received the B. App. Sc., M. App. Sc., and Ph.D. degrees from the University of Melbourne, Melbourne, Australia, in 1971, 1973, and 1977, respectively.

From 1976 to 1978, he was a Postdoctoral Research Fellow at Queen Mary College, University of London, London, U.K., followed by five years as a Lecturer in the Department of Electrical Engineering, James Cook University of North Queensland. During 1982 and 1983, he was a Consultant at Plessey Radar, U.K., and in December 1983, he joined CSIRO, Sydney, Australia. He held several positions with CSIRO, culminating with Chief Scientist, ICT Centre. He is currently a CSIRO Fellow and Principal of Antengenuity, a specialist consulting firm, an Adjunct Professor at Macquarie University and a Guest Professor of Shanghai Jiao Tong University..

Dr. Bird is a Fellow of the Australian Academy of Technological and Engineering Sciences, the IEEE, the Institution of Electrical Technology, U.K., and an Honorary Fellow of the Institution of Engineers, Australia. In 1988, 1992, 1995 and 1996 he received the John Madsen Medal of the Institution of Engineers, Australia, for the best paper published annually in the *Journal of Electrical and Electronic Engineering*, Australia, and in 2001 he was co-recipient of the H. A. Wheeler Applications Prize Paper Award of the IEEE Antennas and Propagation Society. Dr Bird was awarded CSIRO Medals in 1990 for the development of an Optus-B satellite spot beam antenna, in 1998 for the multibeam antenna feed system for the Parkes radio telescope and in 2011 for lifetime achievement. He received an IEEE Third Millennium Medal in 2000 for outstanding contributions to the IEEE New South Wales Section. Engineering projects that he played a major role in were given awards by the Society of Satellite Professionals International (New York) in 2004, the Engineers Australia in 2001, and the Communications Research Laboratory, Japan, in 2000. In 2003, he was awarded a Centenary Medal for service to Australian society in telecommunications and also named Professional Engineer of the Year by the Sydney Division of Engineers Australia. He was awarded the M.A. Sargent Medal in 2012 by Engineers Australia for sustained contributions to electrical engineering. His biography is listed in *Who's Who in Australia*.

He was a Distinguished Lecturer for the IEEE Antennas and Propagation Society from 1997 to 1999, Chair of the New South Wales joint AP/MTT Chapter from 1995 to 1998, and again in 2003, Chairman of the 2000 Asia Pacific Microwave Conference, Member of the New South Wales Section Committee from 1995–2005 and was Vice-Chair and Chair of the Section in 1999–2000 and 2001–2002 respectively. Dr Bird was a member of the Administrative Committee of the IEEE Antennas and Propagation Society from 2003–2005, a member of the College of Experts of the Australian Research Council (ARC) from 2006–2007 He was Associate Editor of the IEEE TRANSACTIONS ON ANTENNAS AND PROPAGATION from 2001 to 2004 and Editor-in-Chief from 2004 to 2010. Currently, he is President Elect of the IEEE Antennas & Propagation Society, Chair of the Society's Publication Committee, and a member of the Editorial Boards of the , *Journal of Infrared, Millimeter and Terahertz Waves* and the *IET Microwaves, Antennas & Propagation*.

Y. Jay Guo (SM'96) received the Bachelor Degree and Master Degree from Xidian University, Xi'an, China, in 1982 and 1984, respectively, and the Ph.D. degree from Xian Jiaotong University, China, in 1987. He was awarded an honorary Ph.D. degree in 1997 by the University of Bradford, U.K., for his world leading research in Fresnel antennas.

Currently, he is the Research Director of Advanced Broadband Networks and Services Theme, CSIRO, Australia, and the Director of the Australia China Research Centre for Wireless Communications. From August 2005 to January 2010, he served as the Research Director of the Wireless Technologies Laboratory, CSIRO ICT Centre. Prior to joining CSIRO, he held various senior positions in a number of international companies including Fujitsu, Siemens and NEC, managing the development of advanced technologies for the third generation (3G) mobile communications systems. He is an Adjunct Professor at UNSW, Macquarie University, University of Canberra, Australia, and a Guest Professor at the Chinese Academy of Science (CAS) and Shanghai Jiao Tong University. He has published three technical books *Fresnel Zone Antennas*, *Advances in Mobile Radio Access Networks*, and *Ground-Based Wireless Positioning*, 72 journal papers and over 80 refereed international conference papers. He holds 18 patents in wireless technologies.

Dr. Guo is a Fellow of IET. He was the recipient of the Australian Engineering Excellence Award and the CSIRO Chairman's Medal. He was Chair of the Technical Program Committee (TPC) of 2010 IEEE Wireless Communications and Networking Conference (WCNC) and 2007 IEEE International Symposium on Communications and Information Technologies (ISCIT), and is the TPC Chair of IEEE ISCIT2012. He has been the Executive Chair of Australia China ICT Summit since 2009. He was a Guest Editor of the IEEE TRANSACTIONS ON ANTENNAS AND PROPAGATION, Special Issue on Antennas and Propagation Aspects of 60–90 GHz Wireless Communications. Currently, he is serving as a Senior Guest Editor for the IEEE JOURNAL ON SELECTED AREAS IN COMMUNICATIONS, Special Issue on Challenges and Dynamics for Unmanned Autonomous Vehicles.

Geng Junping (M'09) received the Ph.D. degree in electronic engineering from Northwestern Polytechnic University, Xi'an, China.

From 2003 to 2005, he was a Postdoctoral Researcher with Shanghai Jiao Tong University. He is currently an Associate Professor with the School of Electronic, Information, and Electrical Engineering (SEIEE), Shanghai Jiao Tong University, Shanghai, China. His research interests are antennas, electromagnetic compatibility (EMC), and distributed optic-fiber sensors.